

Article ID: 1003-7837(2005)02,03-0289-05

## Effect of the directional crystallization on microstructure of Ti46Al-5Nb-1W

Vitezslav Smishek<sup>1</sup>, Miroslav Kurska<sup>1</sup>, G. S. Burkhanov<sup>2</sup>

(1. VSB-Technical University of Ostrava, Ostrava-Poruba, Czech republic; 2. Baikov Institute of Metallurgy and Materials Science, Russian Academy of Sciences, Moscow 119991, Russia)

**Abstract:** Ti-Al based intermetallic alloys are promising for various applications in aerospace and automobile industry. Their favorable properties, such as low density and good corrosion resistance, are accompanied on the other hand by low toughness and very difficult metallurgy. One of the possibilities to improve the toughness of Ti-46Al-5Nb-1W (% at. fraction) alloy consists in change of their microstructure into lamellar microstructure, which can be reached moreover by directional crystallization. This experiment is described in this paper. Samples of the Ti-46Al-5Nb-1W (% at. fraction) alloy prepared by plasma and vacuum-induction metallurgy were subjected to directional crystallization. Cooling rates were constant and ranged from  $5.56 \times 10^{-6}$  m/s to  $1.18 \times 10^{-4}$  m/s. Directional crystallization has been accomplished in ceramic tubes made of corundum- $\text{Al}_2\text{O}_3$ . The samples were studied by metallographic and chemical analysis. Lamellar microstructure of the samples was found to consist of  $\alpha_2$ - and  $\gamma$ -phase lamellas. Moreover, ceramic particles  $\text{Al}_2\text{O}_3$  were found to be present in the samples. Distribution of the alloying elements in the samples was homogenous.

CLC number: TG113.12 Document code: A

### 1 Introduction

Topic of intermetallic alloys from the system Ti-Al becomes more and more timely. Ti-Al based alloys find ever broader application thanks to their outstanding mechanical properties and good corrosion resistance even at increased temperatures. This pre-destinates them for application in aircraft and automotive industries, as well as in medicine.

Microstructure of Ti-Al based alloys can achieve these types: equiaxed grains, duplex grains, nearly and fully lamellar grains.

The best combination of strength and toughness from various developed titanium alloys is represented by the alloys with fully lamellar two-phase alloys consisting of TiAl ( $\gamma$ ) and  $\text{Ti}_3\text{Al}$  ( $\alpha_2$ ). Ductility and strength are sensitive to the orientation spacing of lamellas. The best combination of yield stress and room temperature ductility can be achieved when the lamellar orientation is aligned parallel to the tensile axis.

Received date: 2005-08-29

\* Foundation item: Project(106/03/0984) supported by the grant of Grant Agency of the Czech Republic; Project (6198910013) supported by the research plan MSM

Lamellar grains in various microstructures are formed by rotating layers of TiAl and Ti<sub>3</sub>Al<sup>[1, 2]</sup>

We prepared in our laboratory conditions an intermetallic alloy of the system Ti-Al-Me. We chose the alloy with composition Ti-46Al-5Nb-1W (% at fraction). Its chemical composition is given in the table below. We chose niobium as alloying element for this alloy in order to increase resistance to creep. This property belongs to priority ones. It is one of decisive factors for use of material for manufacturing of gas turbine blades or components of diesel engines turbo blowers. Tungsten has the same influence<sup>[3]</sup>.

Table 1 Chemical composition of prepared alloy

Sample designation	Chemical composition (at. fraction) /%			
	Ti	Al	Nb	W
Ti-46Al-5Nb-1W	48	46	5	1

## 2 Experimental

### 2.1 Plasma and vacuum-induction melting

The plasma melting was used to produce ingots in the first step of metallurgical fabrication because of high reactivity of titanium. Titanium reacts with almost all types of high-temperature materials. Plasma furnace is based on the principle of ionization gas. Effective cooling ensures pressure of conduit water, which circulates through tubular crystallizer. There is no soiling by impurities caused by materials of fusion crucible. Low homogeneity is the main disadvantage of this melting method. Composition of ingot noticeably changes along the sectional area. After melting of certain zone by plasma torch there occurs its sharp cooling by water, which passes through a copper crystallizer. Due to this a non-homogenous structure is created. It is possible to ensure higher homogeneity by subsequent re-melting in another type of furnace<sup>[4]</sup>.

In order to increase homogeneity of the alloy we included vacuum-induction melting as the next step in manufacturing process. During melting there occurs intensive mixing by eddy currents, which ensures even distribution of alloying elements. Ingots were re-melted in high-frequency vacuum-induction furnace LEYBOLD-HERAEUS IS1/FFF. During melting there was vacuum in the furnace. The charge was inserted into a corundum crucible stabilized by TiO<sub>2</sub>. This crucible was in graphite tube. As soon as the charge became melted, the furnace was filled with argon. This measure prevented splashing of molten mass from the crucible. Molten mass was poured into graphite ingot-molds. Final form of castings was bar with diameter of 10 mm and length of 100 mm.

### 2.2 Directional crystallization

Directional crystallization was realized in Bridgman type equipment. Top oxidic layer of the sample was turned off. The sample was then inserted into ceramic tube Luxal 203. Directional crystallization was realized under argon protective atmosphere. Argon purity was 4N5. This device consists of heating part of furnace and mobile equipment. Tube with molten mass is fixed to this equipment. In dependence on chosen rate of crystallization, this equipment pulls out the tube with molten mass by constant speed from the furnace hot zone through water-cooled copper mold, and ensures thus the required crystallization of the molten mass in accordance with the pre-set parameters. We chose for the alloy Ti-46Al-5Nb-1W the melting temperature  $T_M = 1680^\circ\text{C}$ . At this temperature there was a dwell lasting 900 s. After this, shifting began. We selected for shifting five constant speeds within the range from  $5.56 \times 10^{-6}$  m/s to  $1.18 \times 10^{-4}$  m/s. After re-

removal of tubes with crystallized melt from the furnace space the samples were taken out and they were longitudinally cut by saw with carbide disc. The samples were then embedded into dentacryl resin and afterwards prepared by grinding and polishing for metallographic observations. Used etching agent consisted of  $\text{HNO}_3$ , HF and distilled water. Etching time varied from 5s to 10s. Observation and taking of pictures were made with use of optical metallographic microscope Olympus GX-51.

### 2.3 Analyses of gases, oxygen, nitrogen

The key issue for envisaged high-temperature applications is the gas contents in material. It can influence very noticeably mechanical properties. That's why we included measurement of gas contents in samples. The samples were cut to dimensions of approx.  $4\text{mm} \times 4\text{mm} \times 5\text{mm}$ . Analyses were made by the Division of laboratories and testing shops at VÚHŽ Dobruška, Czech republic.

Analyses were made on two apparatuses: spectrometric system LECO GDS-750 and analyzer LECO TC-436.

### 2.4 Analyses of particles

Dark particles were present in microstructure of these samples. They were investigated by scanning electron microscope Philips XL 30-EDAX. This analysis proves that these particles are ceramic particles of  $\text{Al}_2\text{O}_3$ .

## 3 Results

Metallographic photos show microstructures of samples melted by selected rates varying from  $5.56 \times 10^{-6}$  m/s to  $1.18 \times 10^{-4}$  m/s. The sections are longitudinal. Microstructure of samples depends on such parameters, as speed of crystallization, which is connected with reaction time and with temperature gradient in molten mass. During the process of directional crystallization we are able to control crystallization of the sample by selection of speed of crystallization. Temperature gradient in molten mass remains still the same. It means that the differences, which are evident in the pictures, reflect various speeds of crystallization. Photos are from samples with rates (a)  $V = 5.56 \times 10^{-6}$  m/s, (b)  $V = 5.56 \times 10^{-5}$  m/s. Speed of solid phase formation is related to it. Fig. 1(a) shows microstructure of the sample of alloy Ti-46Al-5Nb-1W (% at. fraction).

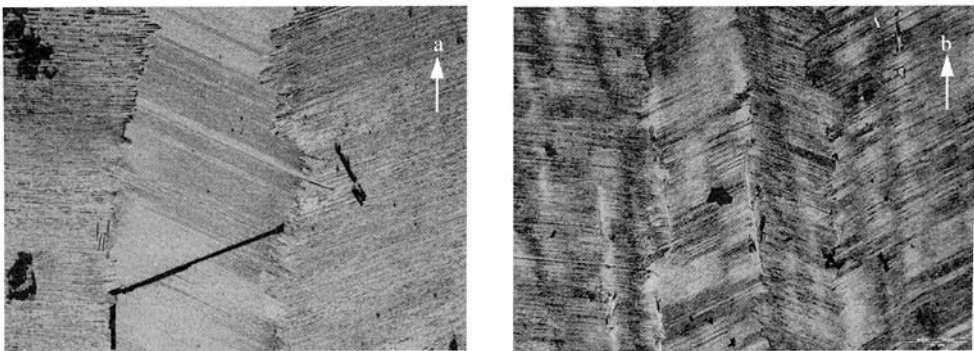


**Fig. 1** Longitudinal section from the sample of the alloy Ti-46Al-5Nb-1W. Dark particles of  $\text{Al}_2\text{O}_3$  are evident. Arrow indicates direction of crystallisation, magnification  $100\times$   
(a)  $V = 5.56 \times 10^{-6}$  m/s; (b)  $V = 5.56 \times 10^{-5}$  m/s

Speed of crystallization was  $5.56 \times 10^{-6}$  m/s. Structure is formed by lamellar grains. Lamellas  $\text{TiAl}$  ( $\gamma$ ) and  $\text{Ti}_3\text{Al}$  ( $\alpha_2$ ) alternate there. These lamellas are oriented predominantly in direction perpendicular to the direction of crystallization. Direction of crystallization is indicated in figures by an arrow, and lamellar grains are oriented in direction of crystallization.

Figure 1 (b) shows photos of microstructure of the same alloy, speed of crystallization  $5.56 \times 10^{-5}$  m/s. In photos there are evident differences in microstructure related to speed of crystallization. The higher the speed, the finer the structure. The other samples with speed of crystallization  $V=1.39 \times 10^{-5}$  m/s,  $V=2.78 \times 10^{-5}$  m/s and  $V=1.18 \times 10^{-4}$  m/s exhibit similar lamellar microstructure, too.

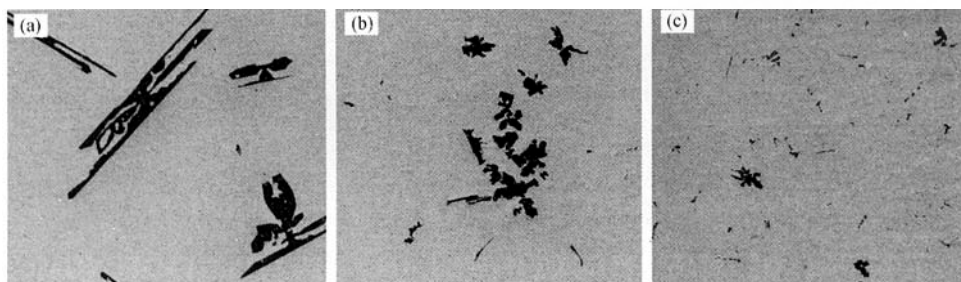


**Fig. 2** Longitudinal sections of samples from the alloy Ti-46Al-5Nb-1W. There are distinct dark particles of  $\text{Al}_2\text{O}_3$ . The arrow indicates direction of crystallisation, magnification  $100\times$   
(a)  $V=5.56 \times 10^{-6}$  m/s; (b)  $V=2.78 \times 10^{-5}$  m/s; (c)  $V=1.18 \times 10^{-4}$  m/s

Inclusions are apparent in structure. It was determined by energy dispersive micro-analyzer EDAX that these are  $\text{Al}_2\text{O}_3$  particles. In the course of melting and crystallization molten mass reacted with ceramic tube. The tube is made of corundum,  $\text{Al}_2\text{O}_3$ . These particles result exactly from this reaction. The difference between density of particles  $\text{Al}_2\text{O}_3$  and density of the alloy Ti-46Al-5Nb-1W is insignificant, that's why the particles float in the molten mass. Thanks to it the moving boundary solidus-liquidus ensured even distribution of these particles. The differences of particles shape are also evident. We can see here particles of slatted form, fine particles and coarse particles, of irregular shape, see Fig. 2. Large slatted particles occurred in the sample with speed of crystallization  $5.56 \times 10^{-6}$  m/s. At the speed of  $2.78 \times 10^{-5}$  m/s the differences in appearance of particles were evident. Shorter reaction time caused different shape and smaller size. The particles developed into clusters. At the speed of  $1.39 \times 10^{-5}$  m/s there are also apparent clusters, but in smaller degree and of smaller size. We can also see here fine dispersed particles.

Number of particles and their dimensions decreased with increasing speed of crystallization. The cause was shorter time for reaction between molten mass and ceramic tube.

Table 2 summarizes contents of gases that were measured in samples. These values show dependence on speed of crystallization. The lower the speed of crystallization, the longer reaction time. This is related to the higher contents of oxygen in molten mass. Contents of oxygen were, however, increased also by pores, which existed in the alloy.

**Table 2 Gas contents in samples**

Sample designation	Crystallization rate /( $\text{m} \cdot \text{s}^{-1}$ )	Oxygen contents (%, mass fraction)	Nitrogen contents (%, mass fraction)
VS-20	$5.56 \times 10^{-6}$	0.4647	0.0013
VS-50	$1.39 \times 10^{-5}$	0.3975	0.001
VS-100	$2.78 \times 10^{-5}$	0.2958	0.00073
VS-200	$5.56 \times 10^{-5}$	0.2714	0.0006
VS-425	$1.18 \times 10^{-4}$	0.2310	0.0004

## 4 Conclusion

The objective of this work consisted in evaluation of influence of directional crystallization on microstructure of the alloy Ti-46Al-5Nb-1W (% at. fraction). Directional crystallization was made by five speeds of crystallization ranging from  $5.56 \times 10^{-6}$  m/s to  $1.18 \times 10^{-4}$  m/s. Changes in microstructure of the alloy were achieved by changing this parameter. The higher the speed of crystallization, the finer the structure. It is formed by lamellar grains, which contain lamellas TiAl ( $\gamma$ ) and  $\text{Ti}_3\text{Al}$  ( $\alpha_2$ ).

During melting and crystallization the alloy reacted with ceramic mold. This reaction resulted in formation of  $\text{Al}_2\text{O}_3$  particles. Distribution of particles in the sample is homogenous. Volumetric part and shape of particles  $\text{Al}_2\text{O}_3$  changed with changing speed. The biggest particles were obtained at the speed of crystallization  $V = 5.56 \times 10^{-6}$  m/s. Distribution of alloying elements was homogenous.

We measured contents of gases-oxygen and nitrogen in the alloy. The measured values show dependence on time, during which the alloy was in molten state. The slower the speed of crystallization, the higher the contents of oxygen and nitrogen.

The presented results were obtained within the frame of solution of the Grant Agency of the Czech Republic, Grant project Nr. 106/03/0984 Metallurgical possibilities of modification of properties of intermetallic compounds from the system Ti-Al and Ti-Al-Me" and of the research plan MSM 6198910013 Processes of preparation and properties of high-purity and structurally defined special materials".

## References

- [1] Saufhoff, G. Intermetallics. VCH Verlagsgesellschaft mbH, d-69451, Weinheim, 1995, pp. 532.
- [2] Szkliniarz, W. Wytwarzanie stop w na osnowie faz miedzymetalicznych z ukladu Ti-Al. In Tytan i jego stopy, conference proceedings, 2002, pp. 167-173.
- [3] Patel P J, Gilde G A, Dehmer P G and Mccauley J W. Transparent Armor. The AMPTIAC Newsletter, vol. 4, no. 3, 2000. pp. 1-19.
- [4] Dembovsk V. Plasma metallurgy. Prague, SNTL, 1978. 259 pages.
- [5] Lapin J, Ondr L. Formation of ceramic particles in intermetallic Ti-46Al-2W-0,5Si alloy during directional solidification. Metallic materials, 2002, vol. 40, No. 3, pp.161-170.
- [6] KucharL, Drápala J. Metallurgy of pure metals. 1<sup>st</sup> ed. Kosice: Nadácia R. Kammela, 2000. 185 pages.